ONLINE FIRST

This is a provisional PDF only. Copyedited and fully formatted version will be made available soon.

ISSN: 0015-5659

e-ISSN: 1644-3284

IGF 1, BDNF, and NGF mediate the neuro-modulatory role of stem cells in acrylamide-induced hippocampal toxic changes in rats

Authors: Nabila Youssef Abdel Halim, Gamal Hosny Mohamed, Ahmed Elhusseiny, Marwa Abdelgwad, Reda Abdelnasser Imam

DOI: 10.5603/fm.101454

Article type: Original article

Submitted: 2024-07-05

Accepted: 2024-09-10

Published online: 2024-09-17

This article has been peer reviewed and published immediately upon acceptance.
It is an open access article, which means that it can be downloaded, printed, and distributed freely, provided the work is properly cited.
Articles in "Folia Morphologica" are listed in PubMed.

ORIGINAL ARTICLE
DOI: 10.5603/fm.101454
Nabila Y. Abdel Halim et al., Stem cells in acrylamide-induced hippocampal neuro-toxic changes

IGF 1, BDNF, and NGF mediate the neuro-modulatory role of stem cells in acrylamide-induced hippocampal toxic changes in rats

Nabila Youssef Abdel Halim[1], Gamal Hosny Mohamed[1], Ahmed Elhusseiny[1], Marwa Abdelgwad[2], Reda Abdelnasser Imam[1]

[1]Department of Anatomy & Embryology, Faculty of Medicine, Cairo University, Cairo, Egypt

[2]Department of Biochemistry, Faculty of Medicine, Cairo University, Cairo, Egypt

Address for correspondence: Reda Abdelnasser Imam, Anatomy & Embryology department, Faculty of Medicine, Cairo University, Cairo, Egypt; e-mail: abdelnasserreada@gmail.com, redabdelnasser@cu.edu.eg

ABSTRACT

Background: Acrylamide (ACR), a common industrial chemical, is a strong neurotoxic material. The hippocampus is a brain area of interest mostly affected by Alzheimer's disease. Mesenchymal stem cells (MSCs) usefulness in various neurological diseases including Alzheimer's is being debated. In this work, the authors aim to explore the role of MSCs in ACR-induced hippocampal neurodegeneration and elucidate the mediating mechanism.

Materials and methods: For this purpose, ten rats served as control, another ten were injected ACR (i.p. 50 mg/kg/day for 2 weeks), and the last ten rats were injected ACR in addition to MSCs (i.p. 1×10^7 MSCs single injection).

Results: ACR induced neurodegenerative histopathological hippocampal changes and adversely altered hippocampal oxidative stress markers SOD, MDA, and GSH. ACR had induced hippocampal demyelination as detected by silver staining. ACR significantly ($P < 0.05$) up-regulated the ELISA hippocampal TNF-alpha and IL-6 and produced microglial & astrocyte activation (as tracked by Iba1 & GFAP immunohistochemistry respectively). ACR significantly reduced hippocampal PCR gene expression of IGF-1 (insulin growth factor-1), BDNF (brain-

derived neurotrophic factor), and NGF (nerve growth factor). MSCs administration had mitigated all the previous deleterious changes.

Conclusions: Acrylamide caused detrimental effects on the hippocampus and demonstrably altered the hippocampal architecture. Bone marrow mesenchymal stem cells offered a promising therapeutic role against these neurotoxic effects of acrylamide, presumably through modulation of IGF 1, BDNF, and NGF gene expressions.

Keywords: acrylamide, stem cells, hippocampus, IGF 1, BDNF, NGF

Introduction

ACR has impaired hippocampal neurogenesis and decreased the hippocampus's neural progenitor cell capacities in young adult mice [15]. Axonal neuropathy, which can impair the central and peripheral nerve systems and is linked to ataxia, weight loss, and skeletal muscle weakness, has been linked to ACR exposure in research studies. The primary pathogenic effects of ACR exposure, in humans, noted were swelling and degeneration of the distal axon fibers [16]. Recent research has highlighted the significance of caspase-1 in a variety of CNS disorders, particularly Alzheimer’s disease, where blood-brain barrier dysfunction is a key factor [19]. ACR exposure produced activation for neuronal Caspase-1 which could be attributed to the activation of the NLRP3 inflammasome within the microglial cells. The activated NLRP3 inflammasome cleaves pro-caspase-1, converting it into its active form, caspase-1, activating IL-1β and IL-18 [33]. The class III intermediate filament GFAP, which is expressed by protoplasmic astrocytes, and the neuroinflammatory marker Iba-1, which is produced by microglial cells, are both elevated during reactive gliosis and widely used as markers of neuroinflammation [13]. ACR exposure leads to demyelination of the cerebellum in rats [8]. This could be attributed to ACR’s ability to reduce levels of key proteins involved in myelination, such as myelin basic protein (MBP), myelin-associated glycoprotein (MAG), and myelin oligodendrocyte glycoprotein (MOG) [25]. After their intraventricular injection in the brain, mesenchymal stem cells (MSCs) can be harvested into brain tissue and develop into supporting glial cells and neurons. Moreover, by expressing neurotrophic factors, MSCs can stimulate primary neural progenitors, enhance the survivability of neural cells, and flexibly differentiate into neural cells [23, 28]. By expressing (BDNF), (NGF), and (IGF-1), MSCs have the potential to stimulate neurogenesis and inhibit apoptosis in

the tissues they are transferred to. Accordingly, several neurodegenerative illnesses, including Alzheimer's disease have been argued as potential targets for therapy with MSCs [14]. In this work, we tried to elucidate the mediating role of (Caspase-1, BDNF, IGF-1, NGF, astrocytes, and microglial cell activation) in MSCs modulation of ACR-induced hippocampal neurodegeneration.

Materials and methods

Chemicals

ACR was obtained from Alpha Chemika, India (Batch no. AC791). 2.4 grams of ACR powder were dissolved in 240 mL 0.9% saline to achieve a 10 mg/mL concentration. Caspase-1 rabbit polyclonal antibody (catalog no. GB11383, Service bio), GFAP polyclonal Antibody (catalog no. GB11096, Service Bio), Iba-1 polyclonal antibody (catalog no. A3160, AB clonal technology). Glutathione peroxidase (GPx) (Biodiagnostic CAT. No. GP 2524), superoxide dismutase (SOD) (SolarBio, Cat No: BC0170), and malondialdehyde (MDA) (SolarBio, Cat No: BC0170). The ELISA kits for IL-6 and TNF-α (tumor necrosis factor alpha) were provided by ELK Biotechnology CO., LTD, Wuhan, China; Interleukin-6 (Cat: ELK1158) and TNF-alpha (Cat: ELK1396). The kit used for RNA extraction was purchased from Thermo Fisher Scientific Inc., Dreieich, Germany (GeneJET, Kit, #K0732), The kit used for PCR was supplied by ELK Biotechnology CO., LTD, Wuhan, China (One Step SYBR Green RT-PCRMix, catalog no. EQ007-02)

Animals

The Animal Ethical Committee of Cairo University ((IACUC) approved thirty Wistar albino rats weighing 150-200 g for usage in this research under approval number CU-III-F-11-22, with performing the experiment at the animal house, faculty of Medicine. The rats were given two weeks to acclimatize before starting the experiment and allowed free access to standard food and water ad libitum. They were divided into the following groups:

1) **The control group** received saline for two weeks, and the ACR group received intraperitoneal ACR at 50 mg/kg/day for 2 weeks (1 mL of prepared solution for each rat/day). To decrease the degree of stress experienced by the rats, the procedure was

performed for three days in a row, followed by a day of rest (total 12 doses in 2 weeks) [15],

2) **ACR + MSCs group:** received ACR for 2 weeks (similar to group 2), then rats were further injected, intra peritoneally, once with MSCs (1×10^7 MSCs suspended in 0.2 mL physiological saline) at the beginning of the 3rd week. The experiment ended four weeks after the stoppage of ACR or saline administration [9].

MSCs preparation

Bone marrow was harvested from the tibias of albino rats by flushing with phosphate-buffered saline (PBS). 15 mL of the flushed bone marrow cells were carefully layered onto an equal volume of Ficoll-Paque (Gibco-Invitrogen, Grand Island, NY, USA) and subjected to centrifugation at 400 × g for 35 minutes. The isolated bone marrow-derived mesenchymal stem cells (BM-MSCs) were cultivated and expanded in 25 mL culture flasks using Roswell Park Memorial Institute (RPMI)-1640 medium enriched with 10% fetal bovine serum and 0.5% penicillin and streptomycin. The cultures were incubated at 37 degrees Celsius with 5% carbon dioxide for 12 to 14 days, with media replacement every 2 to 3 days. Once substantial colonies formed, the cultures were rinsed twice with PBS and treated with 0.25% trypsin containing 1 mL EDTA for 5 minutes at 37 degrees Celsius. Following centrifugation, the cell pellets were resuspended in a serum-supplemented medium and transferred to a 50 cm^2 culture flask (Falcon). These cultures were designated as first-passage cultures. Cultured MSCs were characterized by their morphology and also by the flow cytometry performed via fluorescence-activated cell sorting (FACS) to assess their reaction to (CD105, 29, 34, 45). FACS was carried out at Pathology Unit in Abo El-Rish Hospital (Cairo University Pediatric Hospital).

Histological study

The rats were sacrificed by intraperitoneal injection of 80 μg/g body weight phenobarbitone sodium at the end of the experiment. Each rat was decapitated around just rostral to the first cervical vertebra. The brain was extracted after occipital, parietal, temporal, and frontal bone removal. The brain was sliced along the median longitudinal fissure into the two cerebral hemispheres, one cerebral hemisphere was fixed in a test tube containing neutral buffered 10% formaldehyde for histological and immuno-histochemical processing, while the other hemisphere

was further dissected to extract the hippocampus for biochemical and gene expression studies. Cerebral hemisphere sections at the hippocampus were paraffin-blocked and stained with HE and silver. For silver staining, deparaffinization was done and sections were hydrated and washed, placed in silver nitrate, concentrated ammonium hydroxide was added, and sections were washed in 0.1% ammonium hydroxide, 350 μL of developer solution (0.2 mL 37% formaldehyde, 12 mL dH2O, 12.5 μL 20% nitric acid and 0.05 g citric acid) was added, sections were until changed black, the reaction was stopped using hypo (5% sodium thiosulfate) for 5 minutes.

Immunohistochemical study

Deparaffinized sections underwent heat-induced Epitope Retrieval (HIER) utilizing Cell Marque trilogy with enhancement by heating in citrate buffer PH (6.0). After that, peroxidase activity was counteracted by 3% hydrogen peroxide. This was followed by incubating the tissue sections with antibodies for 60 minutes against active Caspase-1 rabbit polyclonal antibody (1:100), GFAP polyclonal Antibody (1:100), Iba-1 polyclonal antibody (1:200). The slides were incubated with UltraVision One HRP Polymer, and Substrate/Chromogen was prepared. Slides were placed in a DAB substrate, followed by counterstaining with hematoxylin.

Histomorphometric study

Image J Processing and Analysis in Java image analyzer program was used to collect quantitative data from the slides obtained. Microscopic five non-overlapping fields were obtained randomly from each slide, examined in a measuring frame at magnification 400× and the mean values were obtained. The following parameters were quantified: Cell count of CA1, CA2, and CA3 Pyramidal as well as DG granular neurons in HE stained sections, the optical density of silver in CA1, CA2, CA3, and DG regions in silver-stained sections, area percent for each of; GFAP, caspase-1 and Iba-1 immune-reactivity in immune-stained sections.

Biochemical study

The hippocampus was preserved in 0.1M phosphate buffer saline (PBS) solution and underwent centrifugation for 10 minutes at 1200 rate/minute. The supernatant was used to determine the tissue level of GPX, SOD, MDA, (IL-6), and (TNF-α).

a) Assessment of GPX, SOD, and MD by colorimetry. Manufacturer's instructions were strictly followed.
b) ELISA technique was used to assess (IL-6), and (TNF-α) where Manufacturer’s instructions were strictly followed
c) For the Molecular study (gene expression of IGF 1, BDNF, and NGF by real-time PCR), Thirty mg of hippocampal tissue samples were homogenized in RNA extraction buffer to complete RNA extraction assay, lysate transferal was performed to the GeneJET RNA purification column, The yield of total RNA obtained was determined spectrophotometrically at 260 nm. For the Quantitative real-time PCR assessment, data were represented as in Cycle threshold (Ct) for assessed genes (IGF-1, BDNF and NGF) and the housekeeping gene (GAPDH). The relative expression of each target gene is quantified according to the calculation of delta-delta Ct (ΔΔCt). The primer sequences of the IGF 1, BDNF, and NGF genes are illustrated in Table 1.

Statistical analysis

All data values of this research were statistically analyzed using GraphPad Prism version 10, with An (ANOVA) (one-way analysis of variance) test performed for comparison between different groups. Post hoc t-test was used to compare every two different groups, where p-values cut-off was ≤ 0.05.

Results

Clinical observations

Although the ACR group of rats exhibited a general decrease in behavior and well-being, no mortality was recorded among all groups of rats.

Characterization of stem cells

MSCs were identified by their fusiform and spindle shape with a branching pattern in the culture media as shown in phase contrast microscopy. MSCs exhibited –ve expression for CD34 and CD45, whereas exhibited +ve expression for CD29 and CD105 when tracked by flow cytometry (Figure 1).

Level of oxidant/antioxidant markers (Table 2)

ACR significantly reduced superoxide dismutase (SOD) and glutathione (GSH), whereas enhanced malondialdehyde (MDA) as compared to the control group. MSCs modulated hippocampal oxidative stress in ACR neurotoxicity: MSCs significantly enhanced SOD and GSH, whereas significantly reduced MDA as compared to the ACR group.

ACR-induced histological changes and the effects of MSCs (Fig. 2)

Upon HE staining, the ACR group showed degeneration and shrinkage of hippocampal neurons in CA1 and CA2, nuclear pyknosis of neurons in CA3, and prominent vacuolations in the DG (dentate gyrus). Hippocampal sections from the stem cell group exhibited degeneration and shrinkage of a few neurons in CA1, normal neurons in CA2, degeneration & shrinkage of a few neurons in CA3, and typical granular neurons in DG. Histomorphometric measurement of pyramidal neurons and granular neurons revealed a remarkable decrease in the ACR group with a reversal of this decrease upon administration of MSCs.

Effect of MSCs on ACR-induced demyelination (Fig. 3)

Upon silver staining, thickened black-stained myelin sheaths were seen in various hippocampal regions in the control group. The ACR group showed decreased myelin content in all regions. Hippocampal sections from the MSCs group showed increased myelin content in different regions. Histomorphometric measurement of the optical density of silver stain in different hippocampus regions revealed a significant decrease in the ACR group with a reversal of this decrease upon administration of MSCs.

Immunohistochemical findings

a) Upon caspase-1 immunohistochemistry, a large number of positively stained hippocampal neurons were observed in different hippocampal regions in the ACR group. The number of positively stained neurons showed a remarkable decrease in the MSCs group. Histomorphometric measurement of the area % of +ve Caspase-1 immuno-stain in different hippocampus regions revealed a noticeable decrease in the ACR group with a reversal of this decrease upon administration of MSCs (Fig. 4).

b) Upon GFAP immunohistochemistry, positively stained astrocytes with many thick branches were observed in large numbers in the various hippocampal regions in the ACR group. Positively stained astrocytes were recorded in a few numbers in the MSCs group. Histomorphometric measurement of the area % of +ve GFAP immuno-stain in different hippocampus regions revealed a marked increase in the ACR group with a reversal of this increase upon administration of MSCs (Fig. 5).

c) Upon Iba-1 immunohistochemistry, positively stained microglial cells in various hippocampal areas were recorded in a few numbers in the control group, whereas observed in large numbers in the toxic group. The number of microglial cells markedly declined in the ACR + MSCs group. Histomorphometric measurement of the area % of +ve Iba-1 immuno-stain in different hippocampus regions revealed a significant decline in the ACR group with a reversal of this decrease upon administration of MSCs (Fig. 6).

Effect of ACR and MSCs on the hippocampal proinflammatory markers (Fig. 7)

ACR remarkably upregulated hippocampal levels of TNF-alpha and Interleukin-6 compared to the control. MSCs significantly downregulated TNF-alpha and Interleukin-6 (IL-6) after ACR-induced neurotoxicity.

Effect of ACR and MSCs on hippocampal gene expression for (BDNF), (NGF), and (IGF-1) (Fig. 7)

ACR remarkably reduced PCR hippocampal levels of (BDNF), (NGF), and (IGF-1). MSCs significantly enhanced PCR (BDNF), (NGF), and (IGF-1) after ACR-induced neurotoxicity.

Discussion

This work elucidated that bone marrow-derived mesenchymal stem cells exhibited remarkable neuromodulatory properties, mitigating ACR-induced neurotoxicity and safeguarding the hippocampal integrity in rats. The present work documented several histological adverse effects of ACR exposure on the hippocampal structure in the form of degeneration and shrinkage of neurons with pyknotic nuclei and intracellular vacuoles. Quantitatively, the study's data showed a significant reduction in the number of pyramidal neurons in CA regions and granular neurons in

the DG of the hippocampi in the ACR groups compared to the control groups. This agrees with a recent study that reported similar findings in rats' hippocampus after exposure to ACR [27]. Silver-stained different regions of the hippocampus of the ACR groups showed significantly decreased optical density denoting a reduced myelination, this is in agreement with the results of a previous study that showed similar effects of ACR exposure on the myelination in the cerebellum of rats [8]. This could be attributed to ACR's ability to reduce levels of key proteins involved in myelination, such as myelin basic protein (MBP), myelin-associated glycoprotein (MAG), and myelin oligodendrocyte glycoprotein (MOG) [25]. Our study confirmed the apoptotic impact of ACR on hippocampal neurons, supporting the results of a previous study that revealed widespread caspase-1 positive cells in CA1, CA3, and DG regions of the hippocampus as well as the frontal cortex of rats exposed to ACR [13]. ACR-induced hippocampal astrogliosis in the present work is complementary to that observed that astroglial cells respond to brain injury by undergoing "reactive astrogliosis", a process whereby astroglial cells undergo cellular hypertrophy and proliferation [22]. Ionized calcium-binding adapter molecule 1 (Iba-1), is a protein that plays a crucial role in the immune response within the central nervous system (CNS). Iba-1 is a marker for microglial activation; hence its upregulation indicates neuroinflammation [17]. Changes in SOD, MDA, and GSH in this study in the ACR group might explain the mechanism by which ACR induces its neurotoxicity based on oxidative stress [7, 32]. Similar findings of PCR results regarding the reduction of brain-derived neurotrophic factor (BDNF) in the ACR were recorded [4]. The downregulation of insulin-like growth factor-1 (IGF-1) mRNA in the ACR groups is contradictory to what was reported as an increase in IGF-1 expression levels on ACR exposure [24]. This might be elucidated by the difference in the dosage used in each study as they used a dose of 25 mg/kg/day while we used a dose of 50mg/kg/day. Another explanation could be that ACR at a lower dose initially triggers a self-defense mechanism in which expression of IGF-1 levels is increased in the early stages of exposure before falling with significant neuronal damage done, further research is still needed to explore the latter explanation. IGF-1 plays a crucial role in both neurogenesis and development, and its association with learning and memory is well-established. Studies in rats lacking IGF-1 demonstrate a reduction in hippocampal synaptic density and number, accompanied by alterations in the distribution and release of synaptic binding proteins and vesicles. These findings collectively highlight the critical contribution of IGF-1 to neuronal connectivity and its potential influence on cognitive functions [30]. The reduction in hippocampal

nerve growth factor (NGF) mRNA expression in the ACR group implies a potential disruption in NGF-mediated neurogenesis and functionality within the hippocampus due to acrylamide exposure. Disagreeing with these findings, ACR was reported to initially stimulate the expression of neurotrophic factors (NGF, BDNF, VEGF, GDNF), suggesting an attempt by neurons to activate self-protective mechanisms [1]. However, the exact mechanism by which the ACR affects NGF gene expression remains not fully understood. Further studies should be conducted to investigate the possible links between the two.

Mesenchymal stem cells have shown abilities as an antiapoptotic agent to protect surviving neurons and inhibit glial scar formation [2]. MSCs injection mitigated cold stress-induced hippocampal histological changes in the CA1 region of the hippocampus [10], supporting the histological findings of the ACR + MSCs in this work. MSCs significantly increased the levels of oligodendrocyte precursor cells, immature oligodendrocytes, and mature oligodendrocytes, creating a favorable environment for myelin regeneration in the brain, including the hippocampus, of rats with experimental autoimmune encephalomyelitis [31]. The latter research augments the present work remyelination effect of MSCs as tracked by silver staining. Further research is needed to fully elucidate the specific mechanisms by which MSCs regulate caspase-1 activity especially its impact on NLRP3. MSCs suppressed inflammasome activation, including the NLRP3 inflammasome, associated with caspase-1 activation. By inhibiting the assembly or activation of inflammasomes, MSCs indirectly downregulate caspase-1 activity, leading to reduced production of IL-1β and IL-18 [6]. Microglia exhibit diverse activation states, categorized as the pro-inflammatory M1 phenotype and the anti-inflammatory M2 phenotype. Notably, it was demonstrated that MSCs can promote the “M1-to-M2” transition in microglia, explaining the observed improvement in neuronal survival in streptozotocin-induced hippocampal impairment [29]. The positive impact of MSCs on hippocampal tissue levels of SOD, MDA, and GSH in this work reflects its antioxidant effect and had been previously reported [3, 21, 11]. The significant reduction of IL-6 and TNF-alpha in the MSCs group was also reported in a similar study found that MSCs significantly reduced IL-6 and TNF-alpha in the hippocampi of rats with neuroinflammation-induced cognitive impairment [20]. MSCs suppress pro-inflammatory responses within the adaptive immune system by releasing prostaglandin E2 (PGE2). This PGE2 binds to receptors on dendritic cells, inducing a shift towards an anti-inflammatory phenotype characterized by increased interleukin-10 (IL-10) secretion. Consequently, the production of pro-

inflammatory cytokines like tumor TNF-alpha and (IL-6) is significantly dampened [5]. MSCs treatment resulted in increased expression of BDNF in the hippocampus of rats exposed to methamphetamine [18], coinciding with the results of this research and giving a therapeutic potential for MSCs in improving cognitive functions. In addition, significant IGF-1 upregulation with MSCs treatment in cerebral ischemia models in rats with middle cerebral artery occlusion [19], agrees with this research results. Furthermore, the observed upregulation of NGF in our stem cell group is consistent with what had been reported that MSCs transplantation mediated anti-apoptotic and neuroprotective effects in a model of hexanedione-induced neuropathy, potentially *via* NGF signaling pathways [27]. A major limitation of this study was inability to inject the stem cells directly intra-ventricularly, therefore further studies are needed to compare the difference between intra-peritoneal and intra-ventricular injection methods of stem cells and measure their concentration in the hippocampus.

Conclusions

Acrylamide caused detrimental effects on the hippocampus and demonstrably altered the hippocampal architecture. Bone marrow mesenchymal stem cells offered a promising therapeutic role against these neurotoxic effects of acrylamide, presumably through modulation of IGF 1, BDNF, and NGF gene expressions.

Article information and declarations

Data availability statement

All data are available upon request.

Ethics statement

The research was approved from IACUC under approval number CU-III-F-11-22.

Author contributions

All authors contributed in data analysis, doing the experiment, editing the manuscript.

Funding

No funds was received for that research.

Acknowledgments

The authors did not receive any financial support.

Conflict of interest

None.

References

1. An S, Shi J, Li Z, et al. The effects of acrylamide-mediated dorsal root ganglion neurons injury on ferroptosis. Hum Exp Toxicol. 2022; 41: 960371221129786, doi: 10.1177/09603271221129786, indexed in Pubmed: 36154307.
2. Andrzejewska A, Dabrowska S, Lukomska B, et al. Mesenchymal stem cells for neurological disorders. Adv Sci (Weinh). 2021; 8(7): 2002944, doi: 10.1002/advs.202002944, indexed in Pubmed: 33854883.
3. Chi H, Guan Y, Li F, et al. The effect of human umbilical cord mesenchymal stromal cells in protection of dopaminergic neurons from apoptosis by reducing oxidative stress in the early stage of a 6-OHDA-induced Parkinson's disease model. Cell Transplant. 2019; 28(1_suppl): 87S–99S, doi: 10.1177/0963689719891134, indexed in Pubmed: 31775521.
4. Erdemli ME, Arif Aladag M, Altinoz E, et al. Acrylamide applied during pregnancy causes the neurotoxic effect by lowering BDNF levels in the fetal brain. Neurotoxicol Teratol. 2018; 67: 37–43, doi: 10.1016/j.ntt.2018.03.005, indexed in Pubmed: 29580927.
5. Fan XL, Zhang Y, Li X, et al. Mechanisms underlying the protective effects of mesenchymal stem cell-based therapy. Cell Mol Life Sci. 2020; 77(14): 2771–2794, doi: 10.1007/s00018-020-03454-6, indexed in Pubmed: 31965214.
6. Gong J, Xiong Z, Yu W, et al. Bone marrow mesenchymal stem cells alleviate acute severe pancreatitis and promote lung repair via inhibiting NLRP3 inflammasome in rat. Dig Dis Sci. 2024; 69(1): 135–147, doi: 10.1007/s10620-023-08189-5, indexed in Pubmed: 38007702.
7. Guo J, Cao X, Hu X, et al. The anti-apoptotic, antioxidant and anti-inflammatory effects of curcumin on acrylamide-induced neurotoxicity in rats. BMC Pharmacol Toxicol. 2020; 21(1): 62, doi: 10.1186/s40360-020-00440-3, indexed in Pubmed: 32811563.
8. Imam RA, Gadallah HN. Acrylamide-induced adverse cerebellar changes in rats: possible oligodendrogenic effect of omega 3 and green tea. Folia Morphol. 2019; 78(3): 564–574, doi: 10.5603/FM.a2018.0105, indexed in Pubmed: 30402879.
9. Kilic S, Yuksel B, Pinarli F, et al. Effect of stem cell application on Asherman syndrome, an experimental rat model. J Assist Reprod Genet. 2014; 31(8): 975–982, doi: 10.1007/s10815-014-0268-2, indexed in Pubmed: 24974357.

10. Kumar SK, Perumal S, Rajagopalan V. Therapeutic effect of bone marrow mesenchymal stem cells on cold stress induced changes in the hippocampus of rats. Neural Regen Res. 2014; 9(19): 1740–1744, doi: 10.4103/1673-5374.143416, indexed in Pubmed: 25422634.

11. Lan XY, Sun ZW, Xu GL, et al. Bone marrow mesenchymal stem cells exert protective effects after ischemic stroke through upregulation of glutathione. Stem Cell Rev Rep. 2022; 18(2): 585–594, doi: 10.1007/s12015-021-10178-y, indexed in Pubmed: 34449012.

12. Li T, Zhang L, Xiong L, et al. Bone marrow mesenchymal stem cells in brain ischemia enhaces axonal regeneration associated with IGF-1. Ibrain. 2019; 5(4): 50–59, doi: 10.1002/j.2769-2795.2019.tb00041.x.

13. Liu Y, Zhang X, Yan D, et al. Chronic acrylamide exposure induced glia cell activation, NLRP3 infl-ammasome upregulation and cognitive impairment. Toxicol Appl Pharmacol. 2020; 393: 114949, doi: 10.1016/j.taap.2020.114949, indexed in Pubmed: 32147541.

14. Noureddini M, Bagheri-Mohammadi S. Adult hippocampal neurogenesis and Alzheimer's disease: novel application of mesenchymal stem cells and their role in hippocampal neurogenesis. Int J Mol Cell Med. 2021; 10(1): 1–10, doi: 10.22088/IJMCM.BUMS.10.1.1, indexed in Pubmed: 34268249.

15. Park HRa, Kim MS, Kim SoJ, et al. Acrylamide induces cell death in neural progenitor cells and impairs hippocampal neurogenesis. Toxicol Lett. 2010; 193(1): 86–93, doi: 10.1016/j.toxlet.2009.12.015, indexed in Pubmed: 20035847.

16. Pennisi M, Malaguarnera G, Puglisi V, et al. Neurotoxicity of acrylamide in exposed workers. Int J Environ Res Public Health. 2013; 10(9): 3843–3854, doi: 10.3390/ijerph10093843, indexed in Pubmed: 23985770.

17. Quan W, Li M, Jiao Ye, et al. Effect of dietary exposure to acrylamide on diabetes-associated cognitive dysfunction from the perspectives of oxidative damage, neuroinflammation, and metabolic disorders. J Agric Food Chem. 2022; 70(14): 4445–4456, doi: 10.1021/acs.jafc.2c00662, indexed in Pubmed: 35364817.

18. Rafaiee R, Ahmadiankia N, Mousavi SA, et al. Bone marrow mesenchymal stem cells improve cognitive impairments induced by methamphetamine in rats and reduce relapse. Bioimpacts. 2023; 13(2): 97–108, doi: 10.34172/bi.2022.23329, indexed in Pubmed: 37193077.

19. Rand D, Cooper I. Caspase-1: an important player and possible target for repair of the blood-brain barrier underlying neurodegeneration. Neural Regen Res. 2021; 16(12): 2390–2392, doi: 10.4103/1673-5374.313031, indexed in Pubmed: 33907012.

20. Skok M, Deryabina O, Lykhmus O, et al. Mesenchymal stem cell application for treatment of neuroinflammation-induced cognitive impairment in mice. Regen Med. 2022; 17(8): 533–546, doi: 10.2217/rme-2021-0168, indexed in Pubmed: 35638401.

21. Stavely R, Nurgali K. The emerging antioxidant paradigm of mesenchymal stem cell therapy. Stem Cells Transl Med. 2020; 9(9): 985–1006, doi: 10.1002/sctm.19-0446, indexed in Pubmed: 32497410.

22. Tabeshpour J, Mehri S, Abnous K, et al. Role of oxidative stress, MAPKinase and apoptosis pathways in the protective effects of thymoquinone against acrylamide-induced central nervous system toxicity in rat. Neurochem Res. 2020; 45(2): 254–267, doi: 10.1007/s11064-019-02908-z, indexed in Pubmed: 31728856.

23. Tfilin M, Sudai E, Merenlender A, et al. Mesenchymal stem cells increase hippocampal neurogenesis and counteract depressive-like behavior. Mol Psychiatry. 2010; 15(12): 1164–1175, doi: 10.1038/mp.2009.110, indexed in Pubmed: 19859069.

24. Thabet NM, Moustafa EM. Protective effect of rutin against brain injury induced by acrylamide or gamma radiation: role of PI3K/AKT/GSK-3β/NRF-2 signalling pathway. Arch Physiol Biochem. 2018; 124(2): 185–193, doi: 10.1080/13813455.2017.1374978, indexed in Pubmed: 28906145.

25. Üremiş MM, Üremiş N, Gül M, et al. Acrylamide, applied during pregnancy and postpartum period in offspring rats, significantly disrupted myelination by decreasing the levels of myelin-related proteins: MBP, MAG, and MOG. Neurochem Res. 2024; 49(3): 617–635, doi: 10.1007/s11064-023-04053-0, indexed in Pubmed: 37989894.

26. Wang Q, Sun G, Gao C, et al. Bone marrow mesenchymal stem cells attenuate 2,5-hexanedione-induced neuronal apoptosis through a NGF/AKT-dependent pathway. Sci Rep. 2016; 6: 34715, doi: 10.1038/srep34715, indexed in Pubmed: 27703213.

27. Wang TB, He Y, Li RC, et al. Rosmarinic acid mitigates acrylamide induced neurotoxicity via suppressing endoplasmic reticulum stress and inflammation in mouse hippocampus. Phytomedicine. 2024; 126: 155448, doi: 10.1016/j.phymed.2024.155448, indexed in Pubmed: 38394736.

28. Zakrzewski W, Dobrzyński M, Szymonowicz M, et al. Stem cells: past, present, and future. Stem Cell Res Ther. 2019; 10(1): 68, doi: 10.1186/s13287-019-1165-5, indexed in Pubmed: 30808416.

29. Zappa Villar MF, López Hanotte J, Pardo J, et al. Mesenchymal stem cells therapy improved the streptozotocin-induced behavioral and hippocampal impairment in rats. Mol Neurobiol. 2020; 57(2): 600–615, doi: 10.1007/s12035-019-01729-z, indexed in Pubmed: 31399955.

30. Zhang Bo, Li H, Wang Y, et al. Mechanism of autophagy mediated by IGF-1 signaling pathway in the neurotoxicity of lead in pubertal rats. Ecotoxicol Environ Saf. 2023; 251: 114557, doi: 10.1016/j.ecoenv.2023.114557, indexed in Pubmed: 36652739.

31. Zhang JM, Wang H, Fan YY, et al. Effect of mesenchymal stem cells transplantation on the changes of oligodendrocyte lineage in rat brain with experimental autoimmune encephalomyelitis. Brain Behav. 2021; 11(2): e01999, doi: 10.1002/brb3.1999, indexed in Pubmed: 33319488.

32. Zhao M, Zhang B, Deng L. The mechanism of acrylamide-induced neurotoxicity: current status and future perspectives. Front Nutr. 2022; 9: 859189, doi: 10.3389/fnut.2022.859189, indexed in Pubmed: 35399689.

33. Zong C, Hasegawa R, Urushitani M, et al. Role of microglial activation and neuroinflammation in neurotoxicity of acrylamide in vivo and in vitro. Arch Toxicol. 2019; 93(7): 2007–2019, doi: 10.1007/s00204-019-02471-0, indexed in Pubmed: 31073625.

Table 1. Primer sequences of all studied genes.

Gene symbol	Primer sequence from 5′- 3′ F: Forward primer, R: Reverse primer
IGF-1	F: CAGTTCGTGTGTGGACCAAG R: TCAGCGGAGCACAGTACATC
BDNF	F: GTCCCTTCTACACTTACCTCTTG R: CTTTGTTTCACCCTTTCCACTCCT
NGF	F: TGCATAGCGTAATGTCCATGTTG R: CTGTGTCAAGGGAATGCTGAA
GAPDH	F: CACCCTGTTGCTGTAGCCATATTC R: GACATCAAGAAGGTGGTGAAGCAG

Table 2. Hippocampal tissue levels of SOD, MDA, and GSH in different groups.

Group	SOD	MDA	GSH
Control	7.284 ± 0.14	7.8174 ± 0.32	69.8201 ± 2.58
ACR	3.372 ± 0.11$^{@}$	53.289 ± 1.05$^{@}$	26.413 ± 2.06$^{@}$
ACR + MSCs	6.517 ± 0.16$^{@,\#}$	21.1661 ± 0.86$^{@,\#}$	81.296 ± 2.36$^{@,\#}$

[@]Significance compared to the control group; [#]Significance compared to the ACR group. ACR — acrylamide; GSH — glutathione; MDA — malondialdehyde; MSCs — mesenchymal stem cells; SOD — superoxide dismutase.

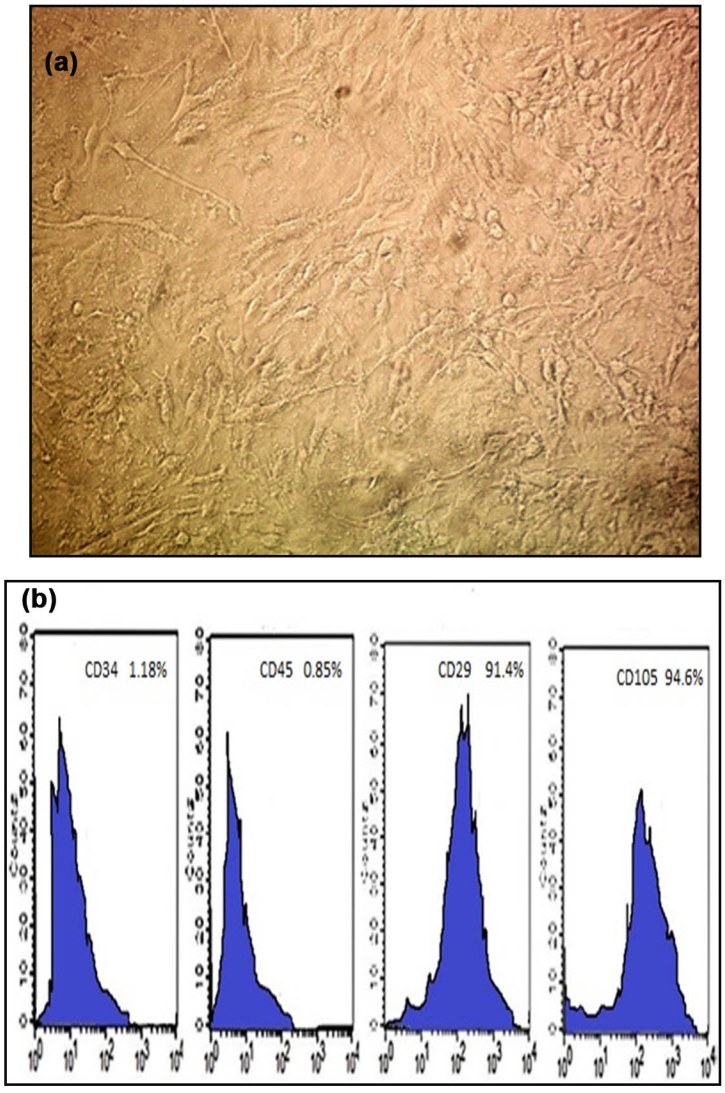

Figure 1A. Photomicrograph from a Phase contrast microscope for MSCs primary culture at 14 days appearing as adhesive fusiform and spindle-shaped cells with a branching pattern. **B.** MSCs

exhibit –ve expression for CD34 and CD45, whereas exhibit +ve expression for CD29 and CD105 when tracked by flow cytometry.

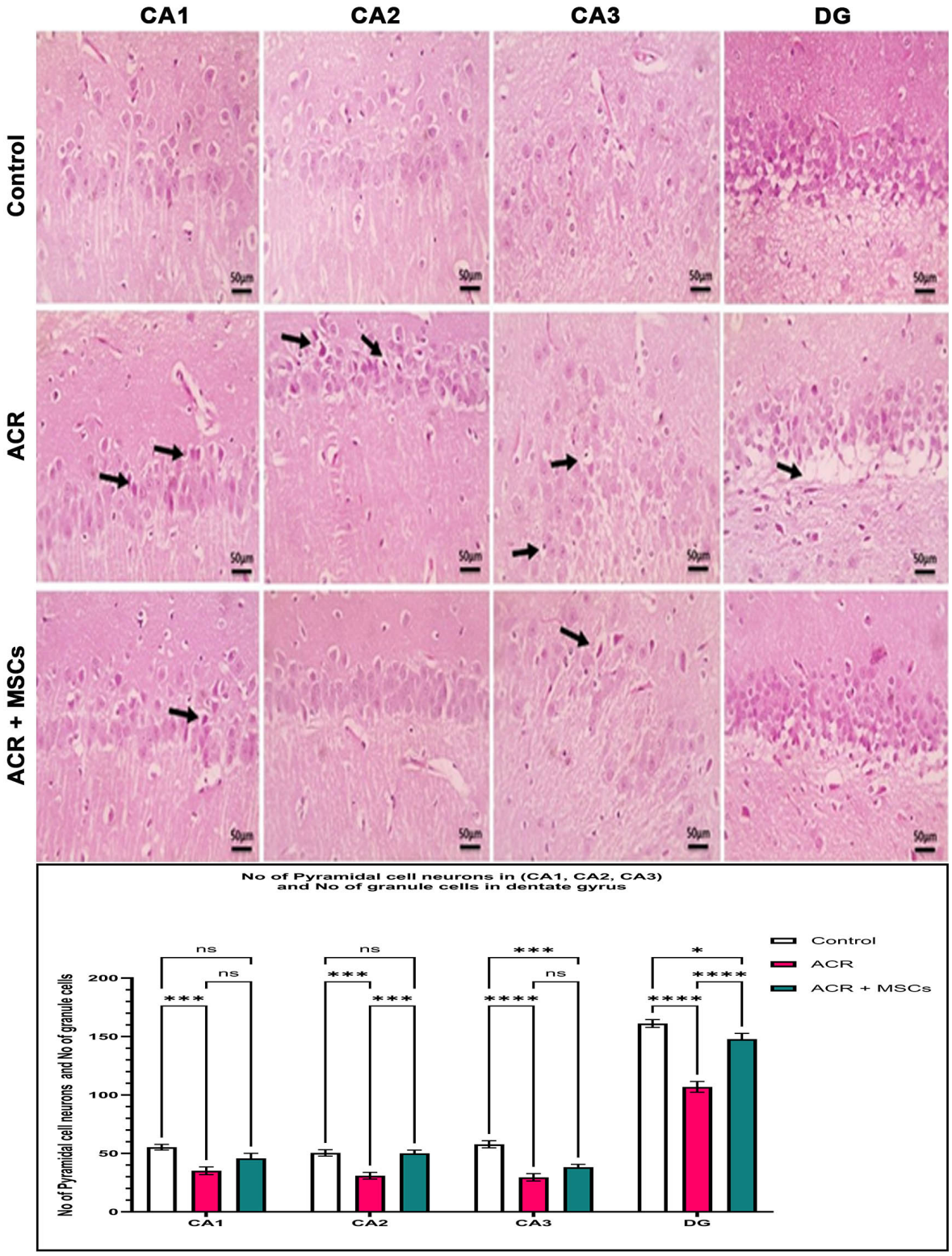

Figure 2. Multiple photomicrographs of the hippocampus highlighting the histological changes in different regions of the hippocampus among different groups. The ACR group shows

degeneration and shrinkage of neurons (black arrows) in CA1 and CA2, nuclear pyknosis of neurons in CA3 (black arrows), and prominent vacuolations (black arrows) in DG (dentate gyrus). Hippocampal sections from the ACR+MSCs group show degeneration and shrinkage of few neurons (black arrows) in CA1, normal neurons in CA2, degeneration and shrinkage of few neurons (black arrows) in CA3, normal neurons granular neurons in DG (HE × 400). The Bar chart shows the difference between the groups regarding the No of pyramidal neurons in CA1, CA2, and CA3 as well as the No of granule cells in DG. The asterisk denotes significance when $P < 0.05$.

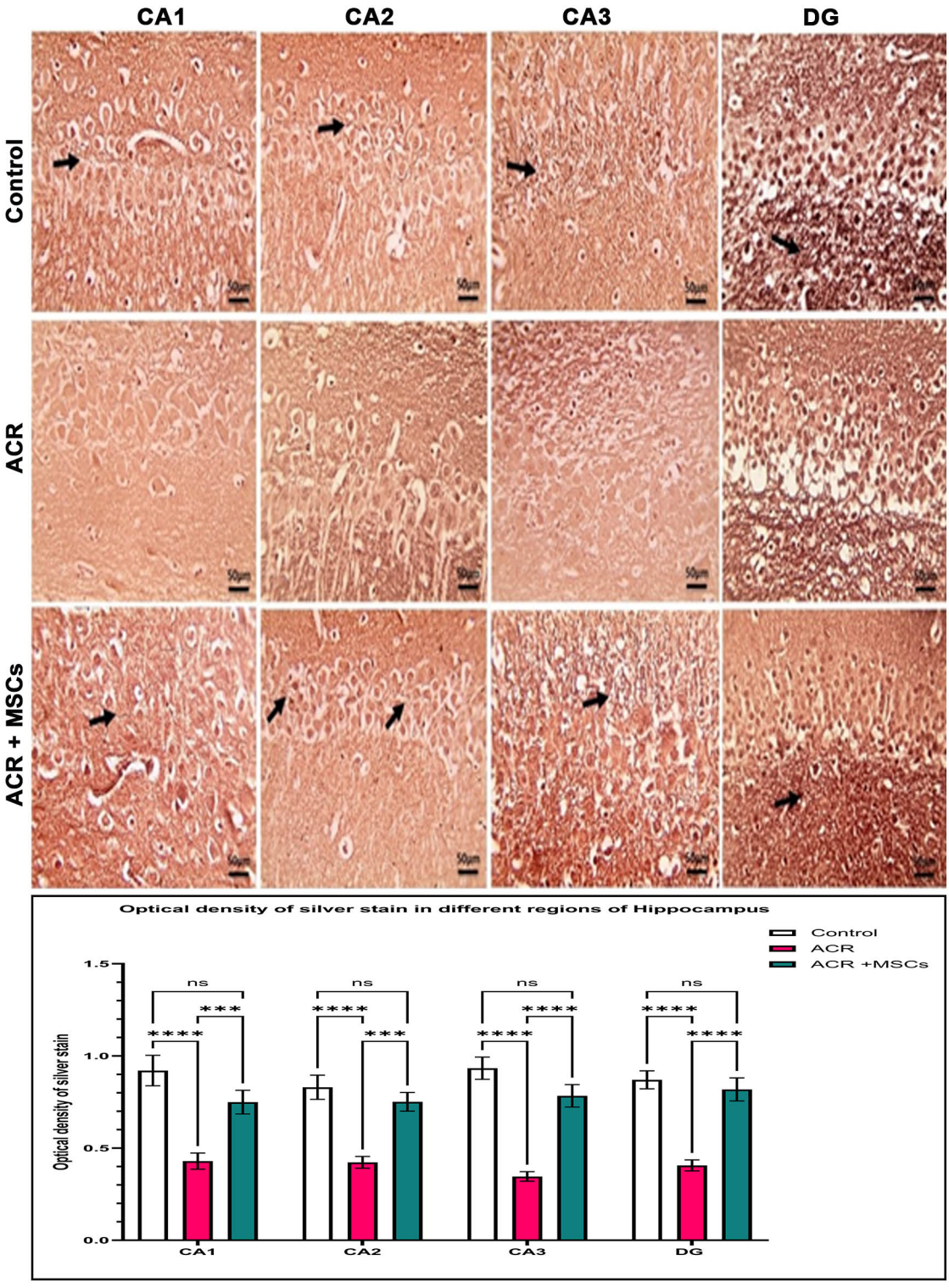

Figure 3. Multiple photomicrographs of the hippocampal sections in different regions among different groups highlighting the myelination changes between the groups. The thickened black-

stained myelin sheath is seen in the control group's CA1, CA2, CA3, and DG (black arrows). Hippocampal sections from the ACR group show decreased myelin content in all regions. Hippocampal sections from the stem group show increased myelin content in different regions (black arrows) (Silver × 400). The Bar chart shows the difference between the groups regarding the optical density of silver stain. The asterisk denotes significance when $P < 0.05$

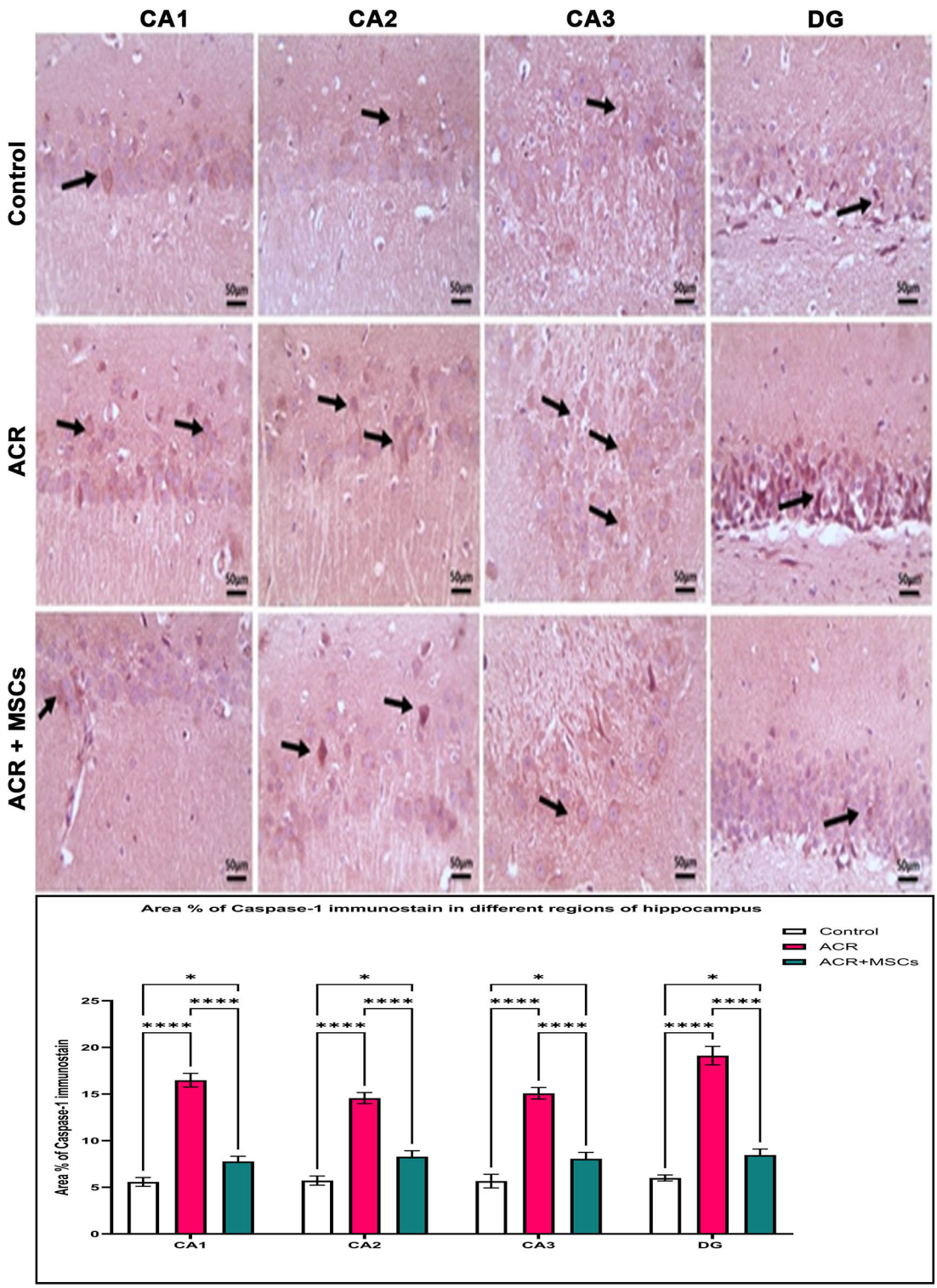

Figure 4. Multiple photomicrographs of immune-stained hippocampal sections against caspase-1 showing highlighting differences in caspase-1 reaction between different groups. A small number

of positively stained neurons are seen in CA1, CA2, CA3 and DG (black arrows) in control groups. Higher numbers of positively stained neurons (black arrows) are observed in ACR groups. The number of positively stained neurons is decreased in the ACR+ MSCs group (Caspase-1 × 400). The Bar chart shows the difference between the groups regarding the area % of positive Caspase-1 immuno-stain. The asterisk denotes significance when $P < 0.05$.

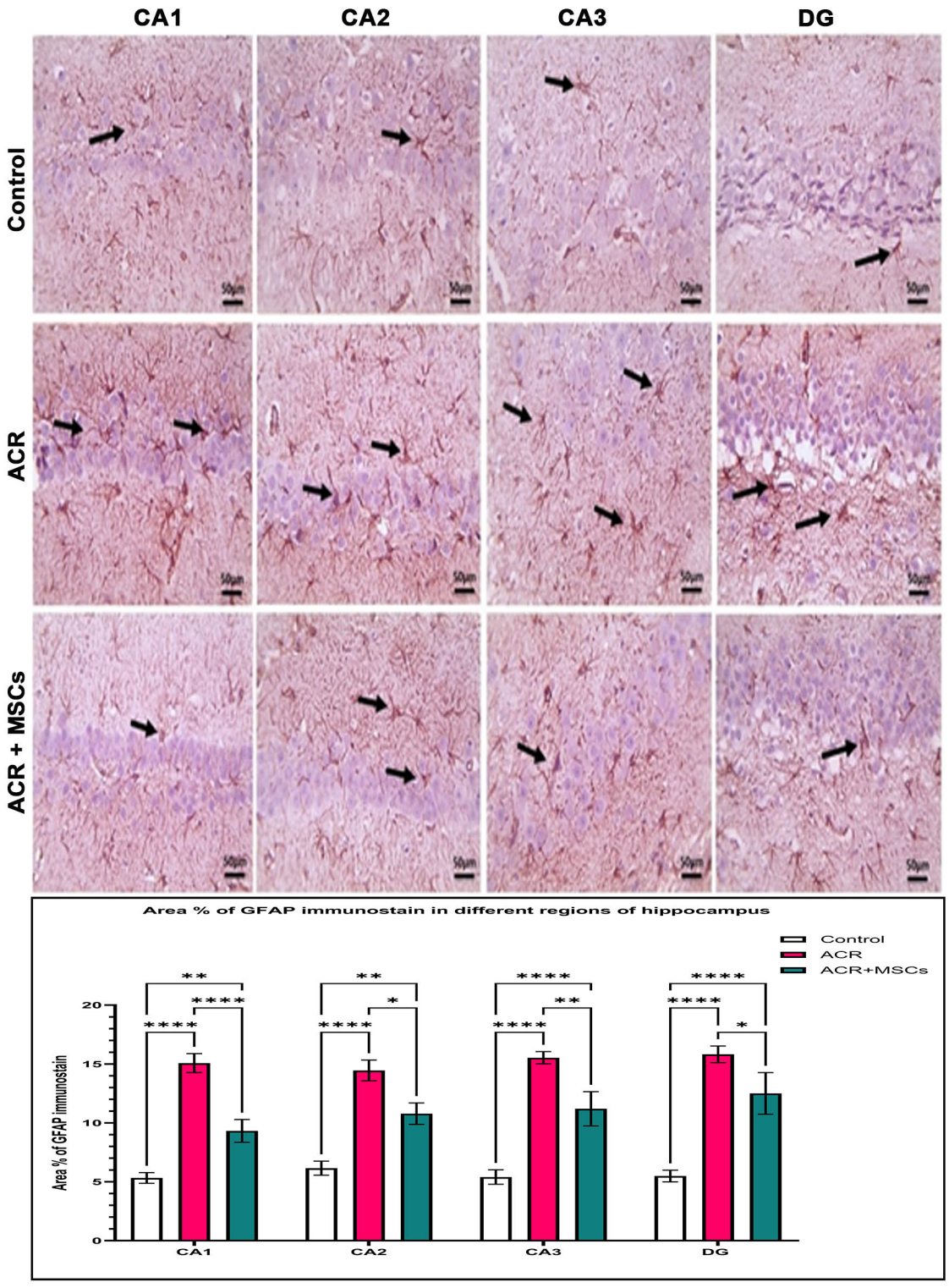

Figure 5. Multiple photomicrographs of immunostained hippocampal sections against GFAP highlighting differences in GFAP positively stained astrocytes between different groups. Few

positively stained astrocytes having few thin branches in CA1, CA2, CA3, and DG (black arrows) are seen in the control group. Higher numbers of positively stained astrocytes having many thick branches (black arrows) are observed in in ACR group. Few numbers of positively stained astrocytes are seen in the MSCs group **(**GFAP × 400). The Bar chart shows the difference between the groups regarding the area % of positive GFAP immuno-stain. The asterisk denotes significance when $P < 0.05$

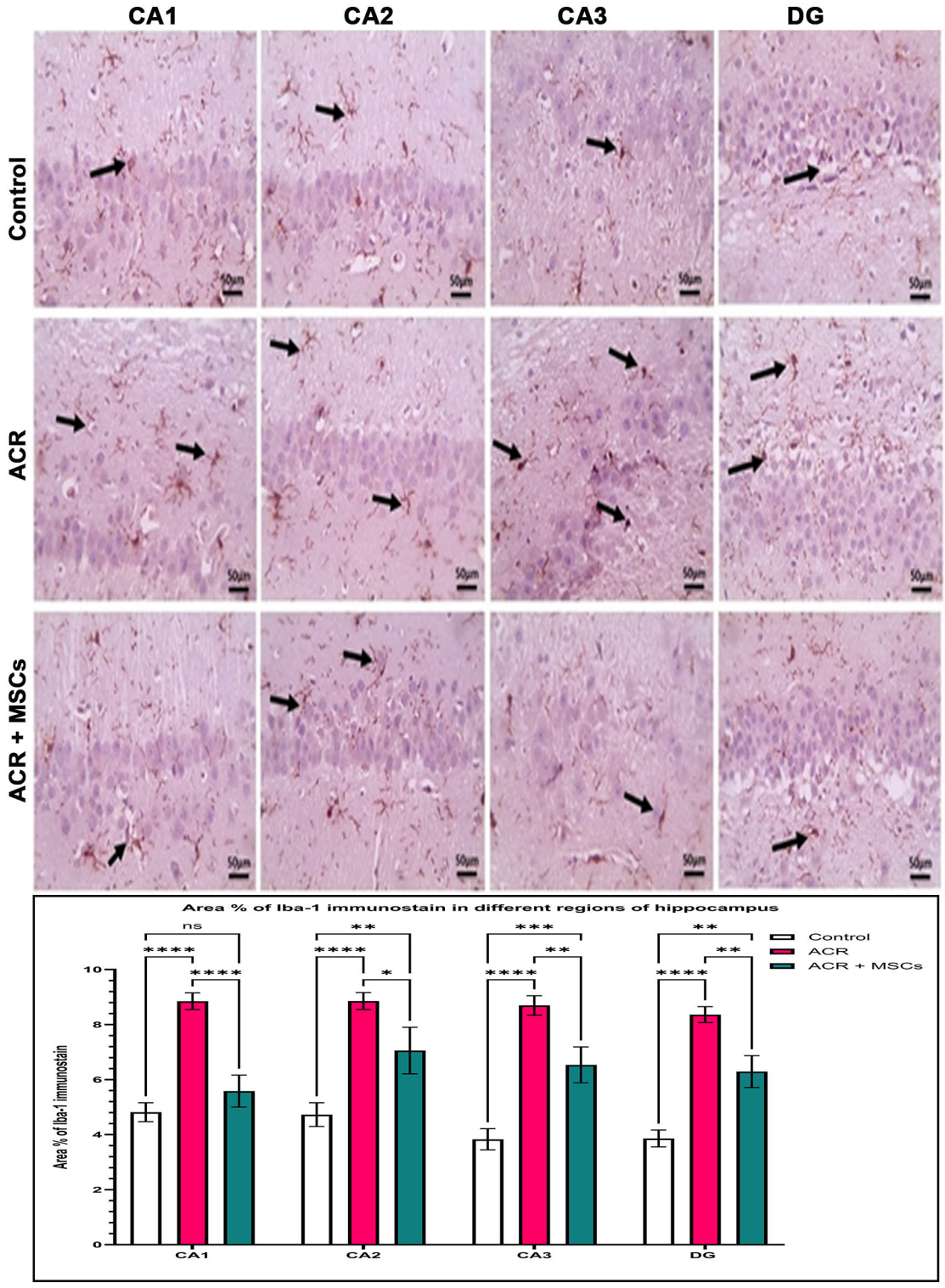

Figure 6. Multiple photomicrographs of immune-stained hippocampal sections against Iba-1 showing few positively stained microglial cells in various hippocampal areas (black arrows) in

the control group. Higher numbers of positively stained microglial cells are observed in various hippocampal areas in the toxic group. The numbers of positively stained microglial cells markedly decreased in CA1, CA2, CA3, and DG (black arrows) in stem cells treated (Iba-1 × 400). The Bar chart shows the difference between the groups regarding the area % of positive Iba-1 immuno-stain. The asterisk denotes significance when $P < 0.05$.

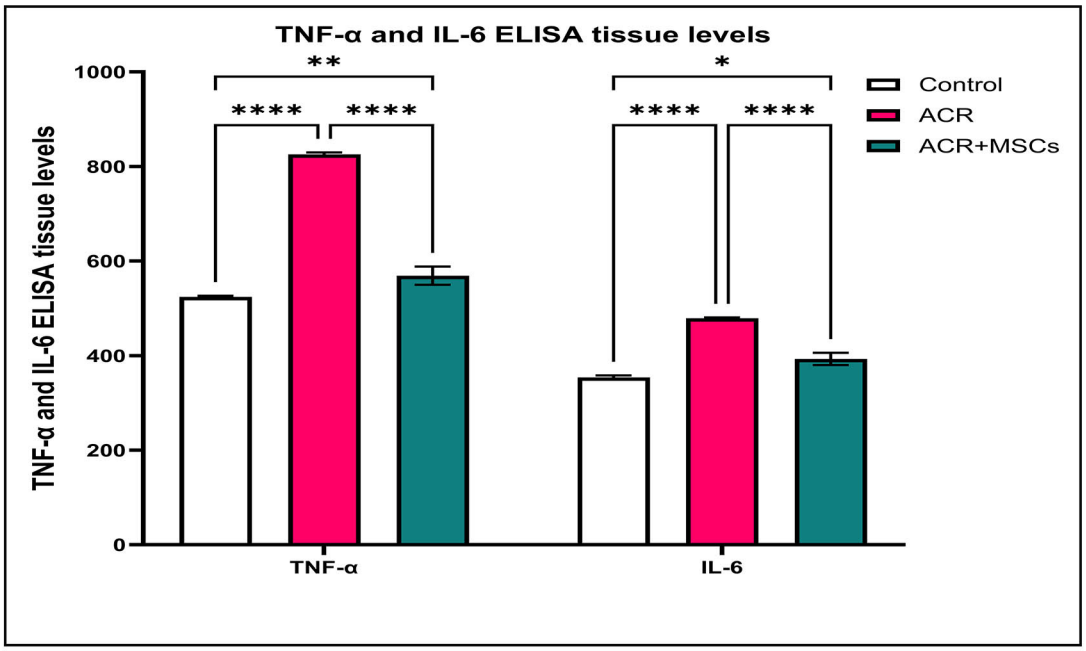
TNF-α and IL-6 ELISA tissue levels
TNF-α and IL-6 ELISA tissue levels
1000
800
600
400
200
0
**
****
****
*
****
****
Control
ACR
ACR+MSCs
TNF-α
IL-6

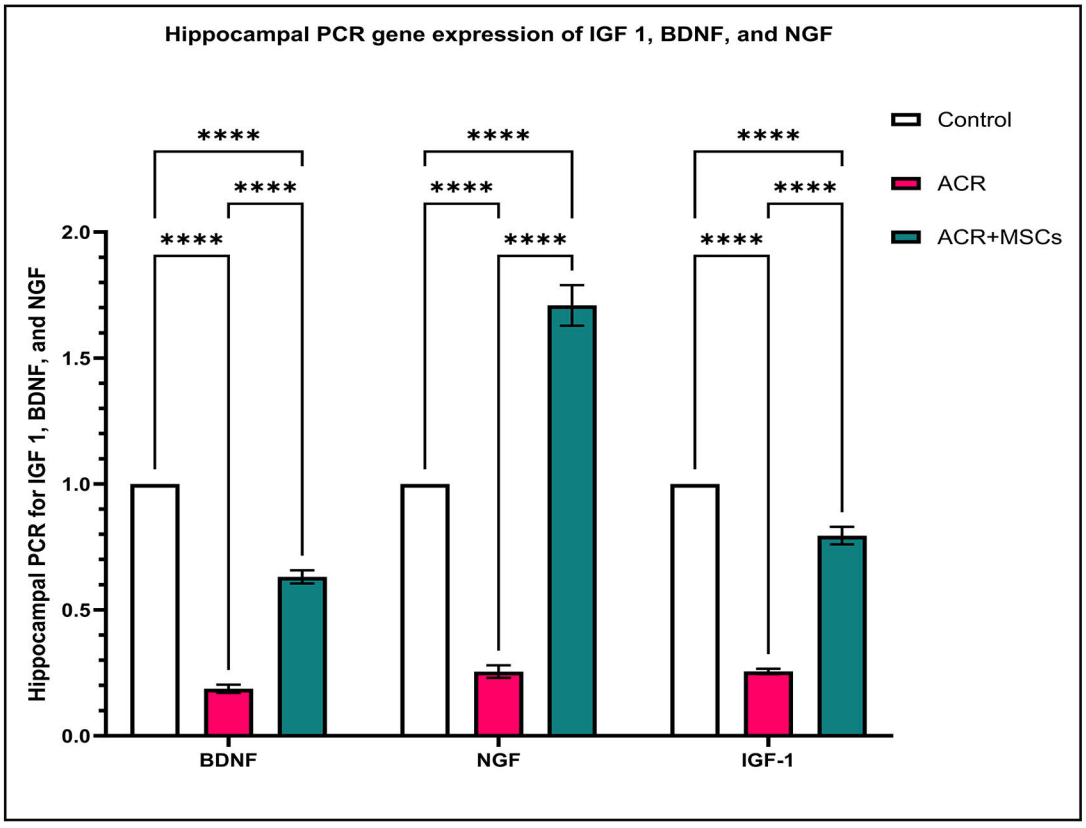
Hippocampal PCR gene expression of IGF 1, BDNF, and NGF
Hippocampal PCR for IGF 1, BDNF, and NGF
2.0
1.5
1.0
0.5
0.0
****
****
****
****
****
****
****
****
****
Control
ACR
ACR+MSCs
BDNF
NGF
IGF-1

Figure 7A. Bar chart for ELISA hippocampal tissue levels of TNF-α and IL-6 in different groups. **B.** Bar chart for PCR hippocampal gene expression for IGF 1, BDNF, and NGF. The asterisk denotes significance when $P < 0.05$.